HARR-JD 69-1201

Chapt. from "The Physics of Se and Te" W. Charles Cooper, Ed., Pergamon Press, Oxford, Eng., 115-34 (1969)

ETCH PIT STUDIES ON SINGLE CRYSTALS OF HEXAGONAL SELENIUM GROWN FROM THE MELT AT HIGH PRESSURES

J. D. HARRISON† and D. E. HARRISON
Westinghouse Research Laboratories, Pittsburgh, Pennsylvania 15235

INTRODUCTION

Recently Harrison and Sagar[1] reported on the use of bromine–methanol solutions for producing well-defined etch pits in the $(10\bar{1}0)$, $(10\bar{1}2)$ and (0001) planes of hexagonal selenium. This paper describes some new etch pit studies on these planes and discusses the relationship between etch pits and defects in the crystals. The etch pits were indexed by the use of the standard projections given in Appendix A which were computed by Hudson and Armstrong.

EXPERIMENTAL PROCEDURE

Etching studies were made on single crystals of hexagonal selenium grown from the melt at high pressures by either random nucleation[2] or seeding.[3] A detailed description of the high-pressure device employed was reported earlier for growth by random nucleation.[2] The seeded growth was done as follows: Beads of "ASARCO" 99.999+ per cent pure selenium were placed in a fused silica vial over a seed crystal. The assembly was inserted into the high-pressure device and air was purged from the system by evacuation and back filling with argon. Using argon as the working fluid, the system was pressurized at from 4000 to 6000 atm. After the system reached steady-state heat flow, the thermal gradient was moved downward until the melting isotherm lay within the selenium seed crystal. The thermal gradient was then moved upward at from 1 to 5 mm/hr, which caused the seed to grow. At the completion of progressive solidification, the heaters were adjusted so that the whole crystal was at a uniform temperature of from 150° to 200°C for several hours. After annealing, the pressure was decreased to 1 atmosphere over a period of from 6 to 60 hr, and the bomb was cooled to room temperature. Upon removal from the high-pressure device, the sample vial was placed in hydrofluoric acid to etch away the fused silica container.

† Present address: Raychem Corp., 300 Constitution Drive, Menlo Park, California 94025.

The $(10\bar{1}0)$ and $(10\bar{1}2)$ surfaces were revealed by cleavage, whereas the (0001) plane was prepared by cutting the crystal with a S.S. White Airbrasive unit followed by grinding and polishing. Since the $\{10\bar{1}0\}$ planes form the primary cleavage system, $\{10\bar{1}2\}$ cleavages were difficult to obtain. Successful $(10\bar{1}2)$ cleavage was assured, however, by first embedding the crystal in an epoxy mounting compound, then cutting a groove through the epoxy encircling the $(10\bar{1}2)$ plane, and finally securing one end of the mounted crystal in a vice and striking the free end with a hammer.

The etchant was made from 5 to 10 vol. per cent analytical reagent bromine dissolved in methanol. After etching, the selenium samples were washed with fresh methanol, then dried with a hot-air blower. Etching times of several minutes caused no staining.

EXPERIMENTAL RESULTS

(a) *Growth Morphology*

Single crystals 1 cm in diameter by 10 cm long with the long axis parallel to either the $\langle 0001 \rangle$ or the $\langle 11\bar{2}0 \rangle$ direction were grown from the melt using pre-oriented seed material. Efforts to seed growth normal to the $(10\bar{1}2)$ face were unsuccessful. Since the $\langle 0001 \rangle$ seeds were easily prepared while the $\langle 11\bar{2}0 \rangle$ seeds were difficult to make, only one crystal was grown in the $\langle 11\bar{2}0 \rangle$ direction. Of the twenty-one crystals grown in the $\langle 0001 \rangle$ direction, all had a polygranular zone above the seed (Fig. 1). In all but three cases, one grain finally dominated to give a single crystal whose crystallographic orientation agreed exactly with the seed. The seed-to-overgrowth continuity was indicated by the simultaneous reflection of the seed, the melt-grown and the vapor-grown crystal sections. A characteristic of the $\langle 0001 \rangle$ crystals was a terminal surface decorated with a forest of vapor-grown needles. Each needle exhibited six specular $(10\bar{1}0)$ faces. Continuity between the seed, the melt-grown and the vapor-grown sections of the crystal was confirmed by Laue back-reflection patterns.

The seeded crystals exhibited smoother, more extensive cleavage on the $(10\bar{1}0)$ planes than those which were randomly nucleated. Prismatic cleavage wafers less than 0.62 mm thick transmitted red light detectable by eye in a darkened room when illuminated with an 18 watt Bausch and Lomb Nicholas Illuminator. Regions of mechanical damage appeared as dark shadows. Most samples thinner than 0.25 mm were translucent, but only about half of those tested between 0.25 and 0.62 mm transmitted red light.

(b) *Included Gas*

Some of the argon which dissolved in the liquid selenium was rejected during solidification. As a consequence, gas bubbles as large as 4 mm in diameter formed at the container–crystal–liquid interface leaving hemispheri-

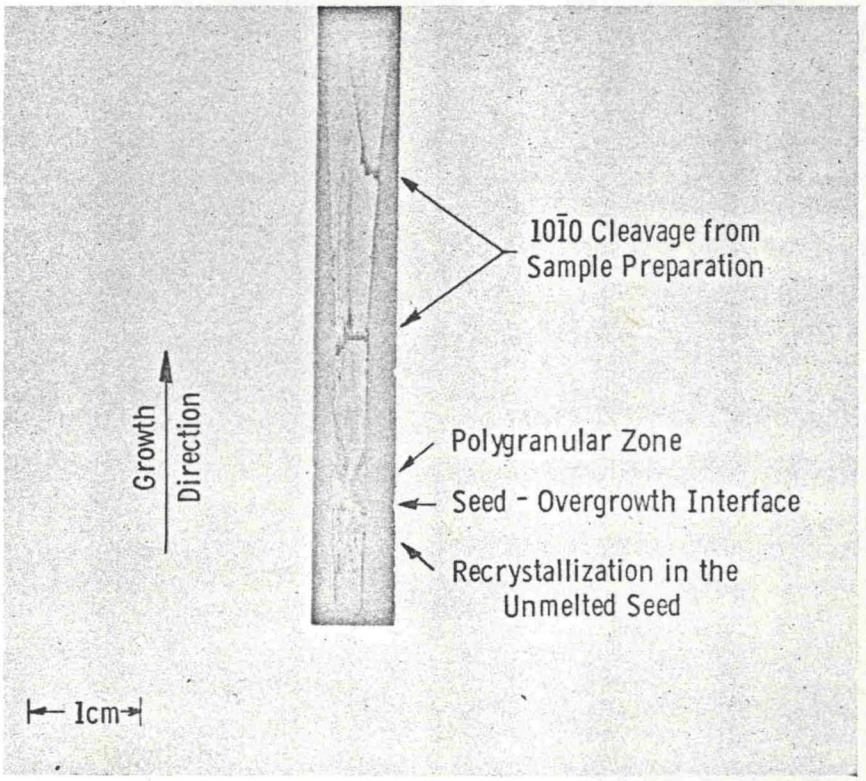

FIG. 1. Sectional view of a seeded 10-mm diameter selenium crystal.

cal marks on the surface of some crystals. In addition, small gas bubbles (from $\frac{1}{20}$ to $\frac{1}{4}$ micron in diameter) formed inside of the 10-mm diameter crystals. Electron micrographs of a replica of a (10$\bar{1}$2) cleavage surface revealed that the outer 2 mm of the crystal was virtually free of bubbles while the density of bubbles in the interior was of the order $10^5/cm^2$. In addition to isolated spheres, hollow pipes which were elongated in the ⟨0001⟩ direction were observed in the (10$\bar{1}$0) cleavage plane. Electron micrographs of replicas of the (10$\bar{1}$2) cleavage surface revealed the presence of hollow pipes as well as isolated spheres. Neither bubbles nor pipes were detected inside of the 3-mm diameter crystals.

(c) *Etch Figures*

The (10$\bar{1}$0) prism surfaces of the 10-mm diameter crystals exhibited three types of etch figures: small, diamond-shaped pits (Fig. 2); large elongated grooves (Fig. 3); and etching steps with scalloped edges (Fig. 3). One diagonal of the diamond-shaped pits was aligned in the ⟨0001⟩ direction and the pits

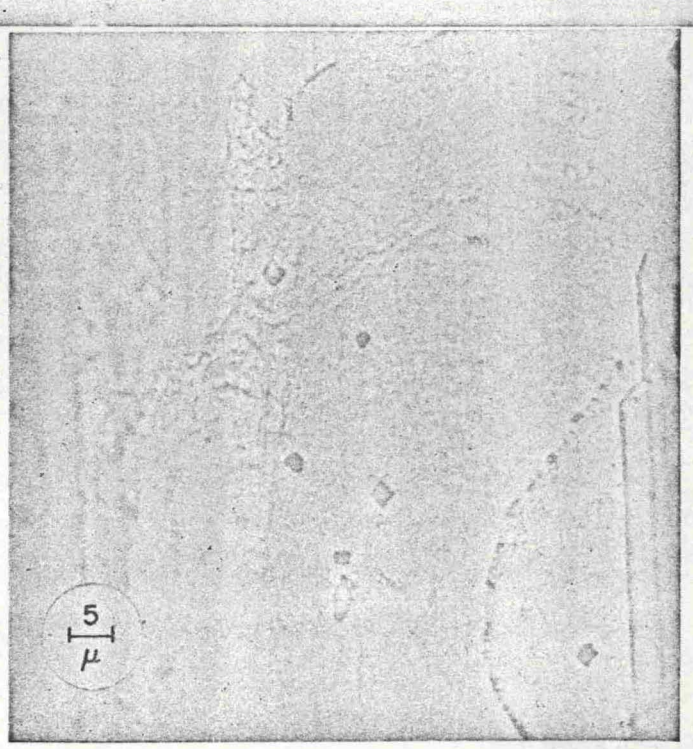

FIG. 2. (10$\bar{1}$0) prism cleavage surface; ⟨0001⟩ direction vertical; etched in 5 vol. % Br in CH_3OH for 8 sec; 10-mm diameter seeded crystal.

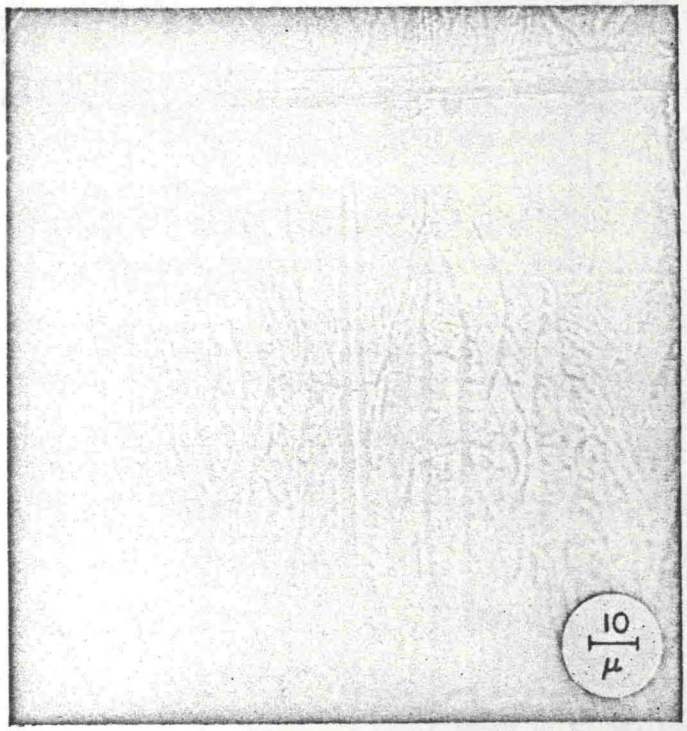

FIG. 3. (10$\bar{1}$0) prism cleavage surface; ⟨0001⟩ direction vertical; etched in 10 vol. % Br in CH_3OH for 4 min; $\simeq 100\ \mu$ removed from surface by etching.

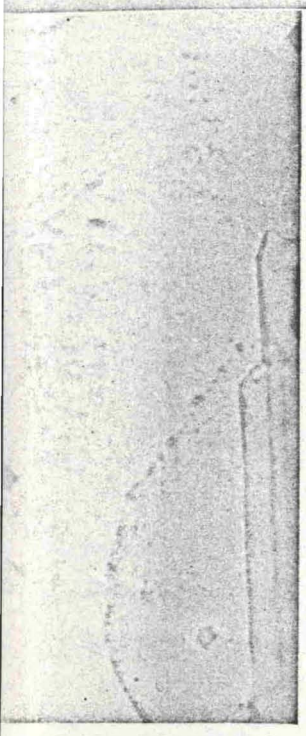

⟨0001⟩ direction vertical; etched in
0-mm diameter seeded crystal.

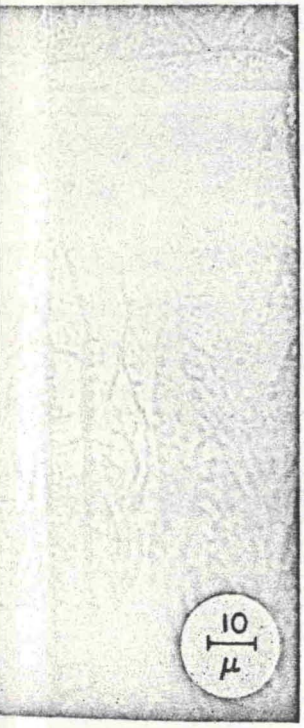

direction vertical; etched in 10 vol,
removed from surface by etching.

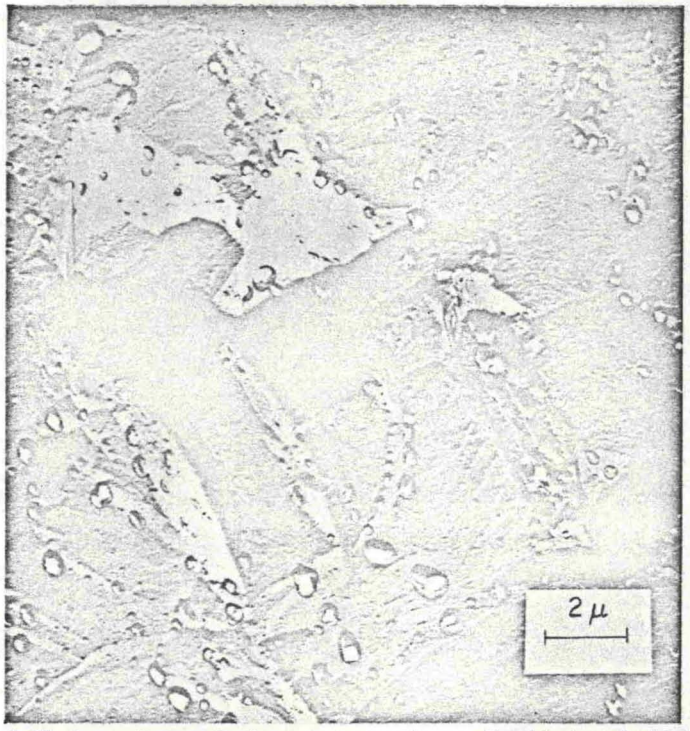

FIG. 4. Electron micrograph of a two-stage carbon replica (shadowed with WO_2 at 45° inclination) from a $(10\bar{1}0)$ cleavage surface etched in 5 vol. % Br in CH_3OH for 30 sec.

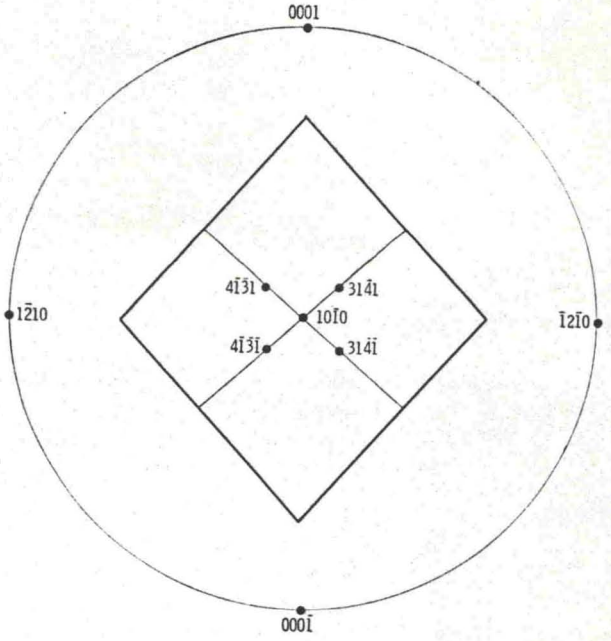

FIG. 5. $(10\bar{1}0)$ pole figure of etch pits in hexagonal selenium.

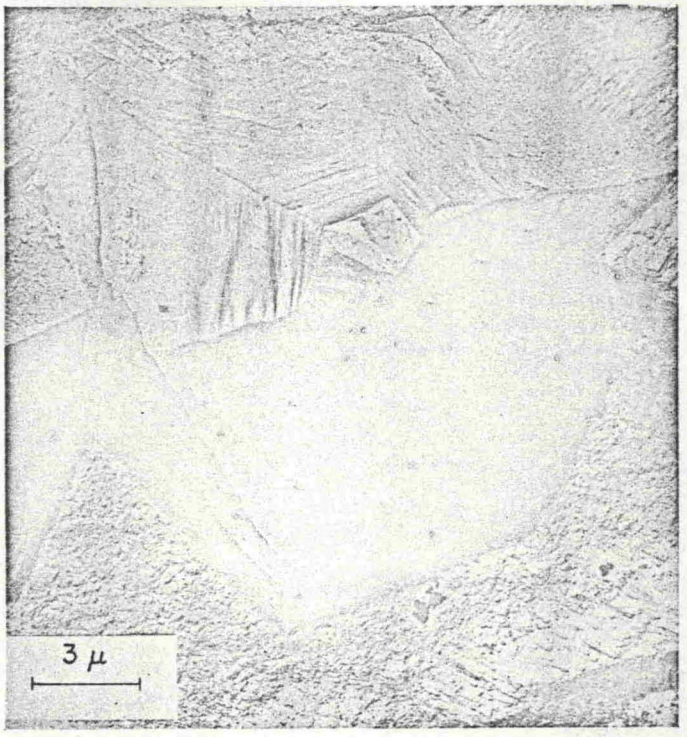

(a)

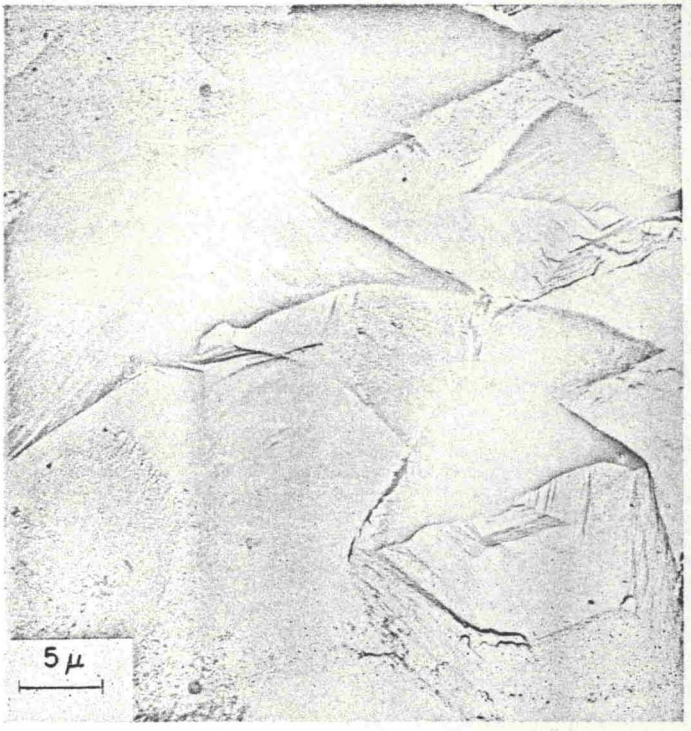

(b)

FIG. 6(a) and (b). Electron micrographs of a two-stage carbon replica (shadowed with WO_3 at 60° inclination) from a (0001) section etched in 5 vol. % Br in CH_3OH for 12 sec.

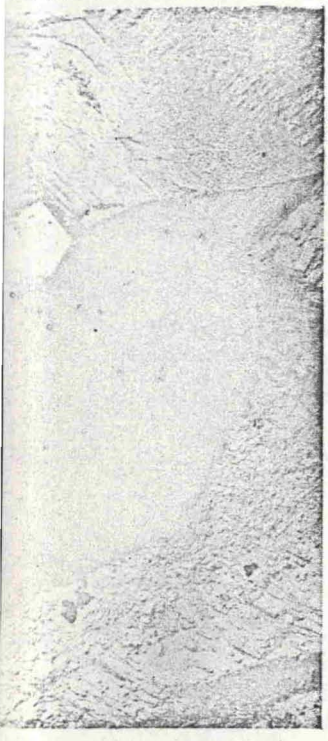



f a two-stage carbon replica (shadowed
001) section etched in 5 vol. % Br in
r 12 sec.

were shallow (Fig. 4). Since the alternate included angles were 85° and 95°, reference to the standard $(10\bar{1}0)$ projection (see Appendix A) indicated that the diamond-shaped pits were bounded by $\{4\bar{1}\bar{3}1\}$ planes as shown by the pole figure in Fig. 5. The elongated grooves which had parallel sides and pointed ends were aligned in the $\langle 0001 \rangle$ direction. As the $(10\bar{1}0)$ surface etched away, old grooves eroded away and new grooves appeared in different locations (see Fig. 3). By contrast, the $(10\bar{1}0)$ cleavage surface of the 3-mm diameter crystals exhibited neither pits nor grooves.

Newly cut, polished and etched (0001) basal plane sections exhibited six-sided pits.[1] Both shallow and deep pits were observed as shown by the electron micrographs in Fig. 6. All of the pits on a particular section had the same geometry, but the pits differed slightly from section to section. The alternate included angles were always 105 and 135 degrees, but the ratio of the length of the short to long sides varied from 1 : 1.4 (see Fig. 7) to 1 : 1 (see Fig. 8). By use of the geometric data and the standard (0001) projection (see Appendix A), the six-sided pits were shown to be formed by the $(30\bar{3}1)$ $(\bar{3}301)$ $(0\bar{3}31)$ and $(13\bar{4}1)$ $(\bar{4}131)$ $(3\bar{4}11)$ planes. This geometry accounts for the observed variation in the ratio of the sides by assuming that the two sets of planes etch at different rates. A pole figure of the 1 : 1.4 and 1 : 1 geometries is shown in Fig. 9. Although the $\{30\bar{3}1\}$ and $\{13\bar{4}1\}$ planes do not converge at a common point, the poles differ by only 2° 20′ from the $\langle 0001 \rangle$ direction.

Freshly cleaved and etched $(10\bar{1}2)$ pyramid planes displayed six-sided pits which, when graphically projected onto the (0001) surface, produced the etch-pit geometry found on the basal plane. All of the six-sided pits on a particular surface had the same geometry, but differences were observed from specimen to specimen. For example, the six-sided pits in the $(10\bar{1}2)$ face of the 10-mm diameter crystal in Fig. 15 had straight sides, whereas the sides of the pits in the $(10\bar{1}2)$ surface of a 3-mm diameter crystal were curved (Fig. 16). Electron micrographs established that some of the pits had flat bottoms while others terminated in long pipes.

(d) *Annealing Effects*

An unexpected result was found upon etching a (0001) section of a 3-mm diameter crystal which had been polished 4 years earlier. Instead of six-sided pits, triangular etch pits which were bisected by the $\langle 11\bar{2}0 \rangle$ direction (Fig. 10) appeared in the basal plane. By means of a two-circle goniometer and the (0001) standard projection, the pits were shown to be formed by the $(2\bar{1}\bar{1}3)$ $(\bar{1}2\bar{1}3)$ $(\bar{1}\bar{1}23)$ planes. A pole figure of the triangular etch pits in relation to the six-sided pits is shown in Fig. 9. Measurements with a two-circle goniometer also revealed that the etching grooves in the $\langle 11\bar{2}0 \rangle$ directions were formed by the $\{10\bar{1}2\}$ planes. After repolishing and etching, the same general distribution of pits reappeared but now the pits were the six-sided $\{30\bar{3}1\}$

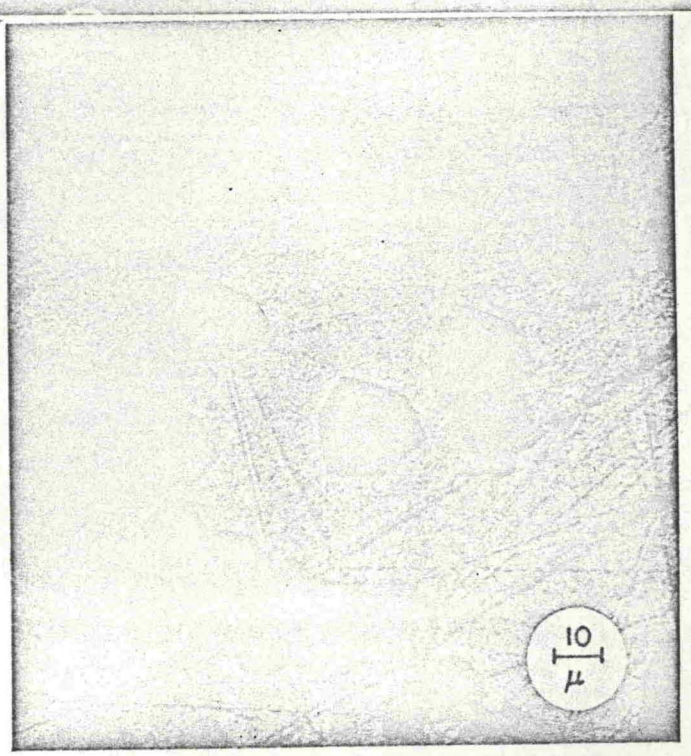

FIG. 7. (0001) basal section prepared by cutting, grinding, and polishing; etched in 5 vol. % Br in CH_3OH for 60 sec; 10-mm diameter seeded crystal.

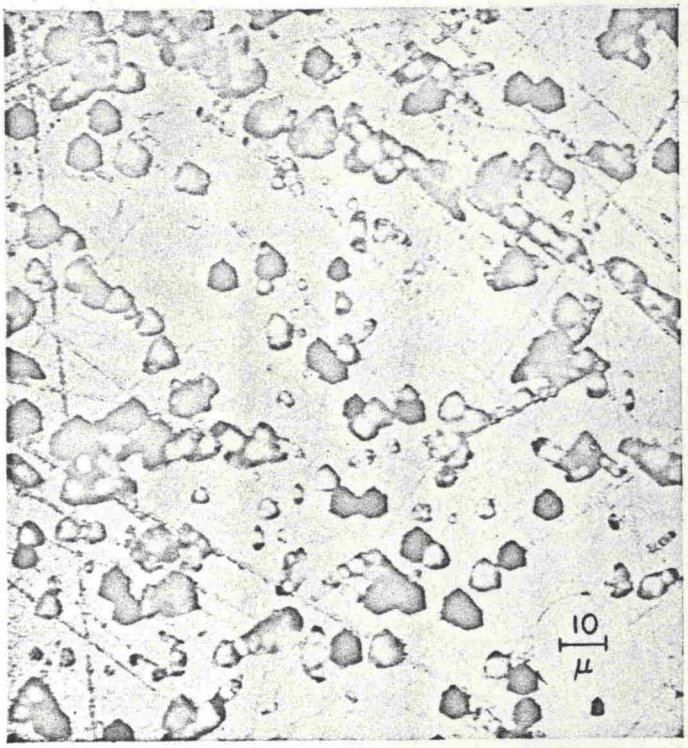

FIG. 8. (0001) basal section prepared by cutting, grinding, and polishing; etched in 5 vol. % Br in CH_3OH for 13 sec; 10-mm diameter seeded crystal.

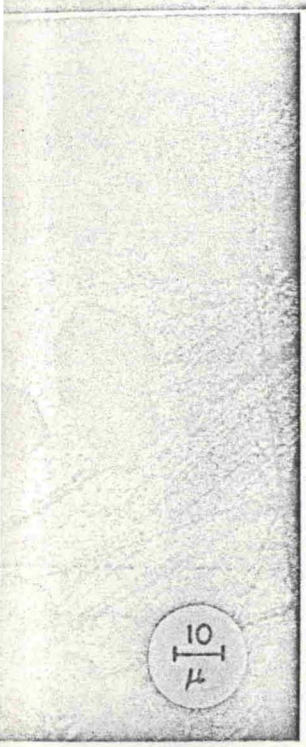

tting, grinding, and polishing; etched
10-mm diameter seeded crystal.

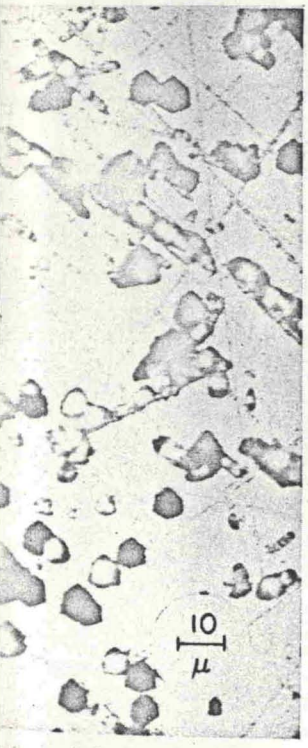

tting, grinding, and polishing; etched
10-mm diameter seeded crystal.

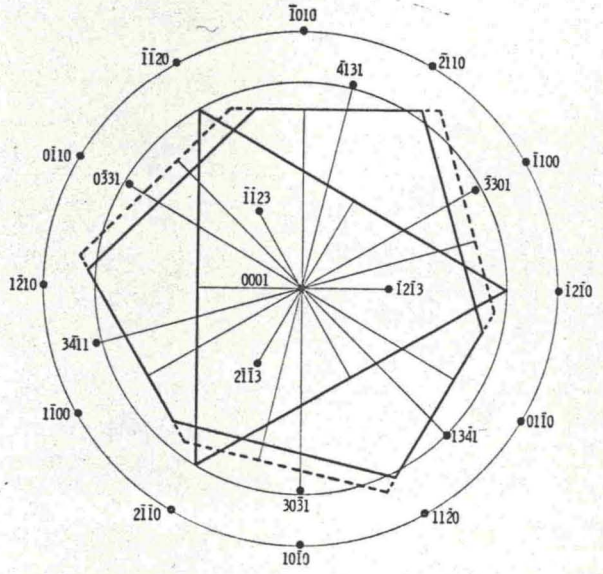

FIG. 9. (0001) pole figure of etch pits in hexagonal selenium.

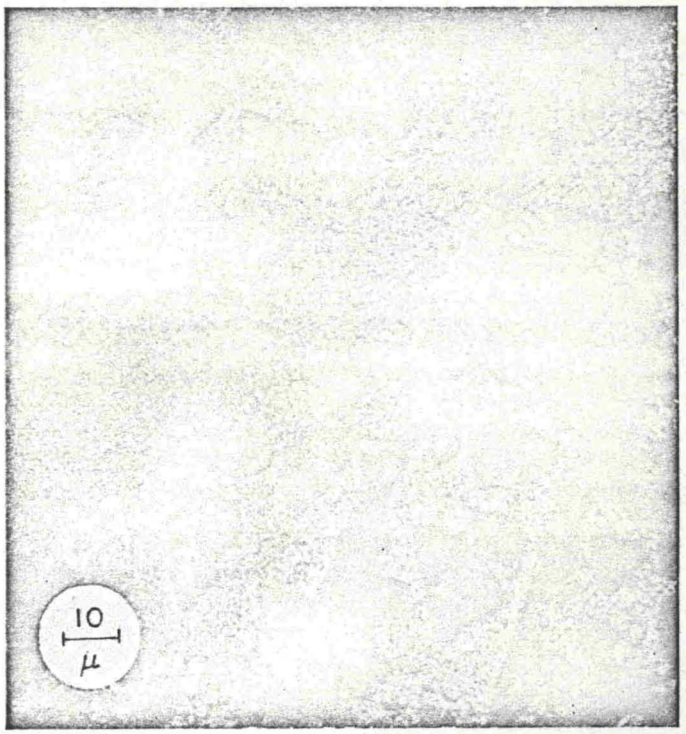

FIG. 10. (0001) basal section prepared by cutting, grinding and polishing; after 4 years surface was etched with 5 vol. % Br in CH_3OH for 80 sec; grooves are in the $\langle 11\bar{2}0 \rangle$ direction; 3-mm diameter crystal grown by random nucleation.

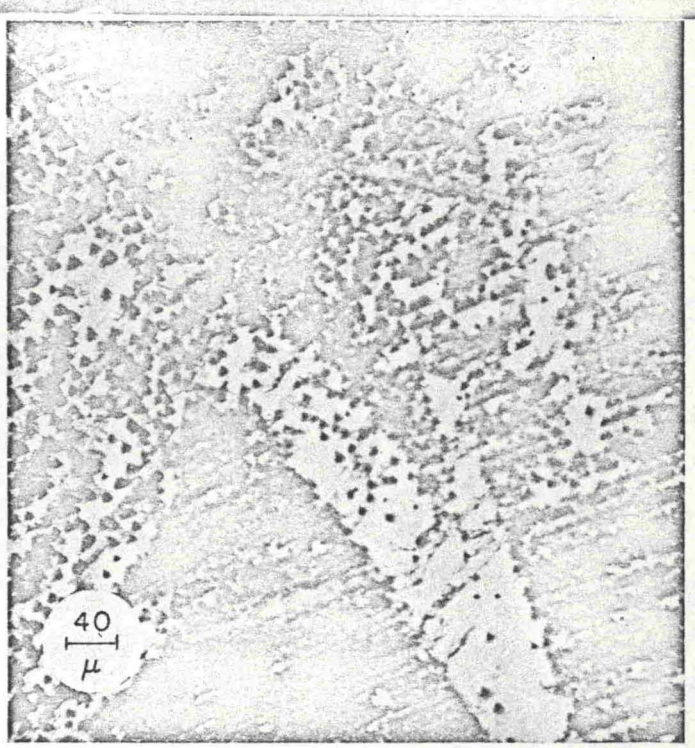

FIG. 11. (0001) basal section prepared by grinding and polishing; after 4 years surface was etched with 5 vol. % Br in CH_3OH for 80 sec; 3-mm diameter crystal grown by random nucleation.

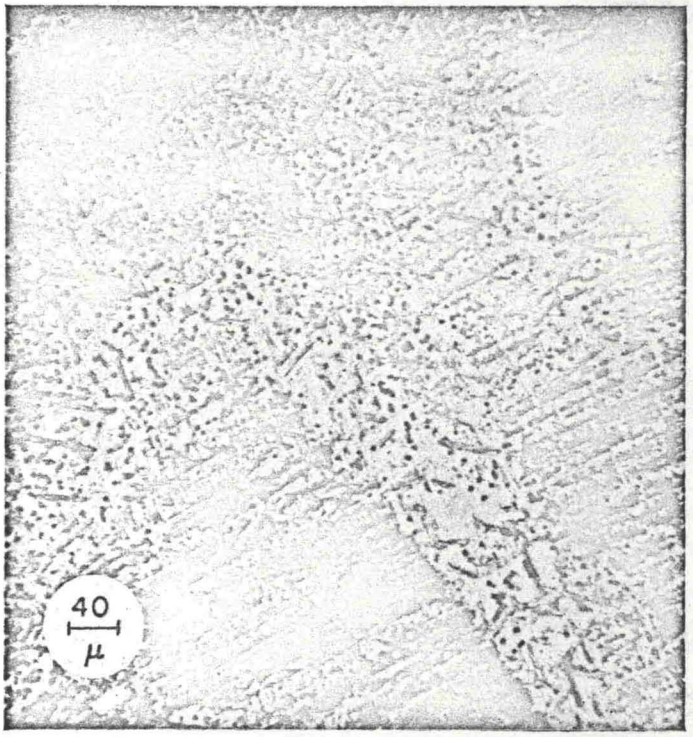

FIG. 12. Repolished and etched (0001) basal section shown in Fig. 11; etched with 5 vol. % Br in CH_3OH for 8 sec.

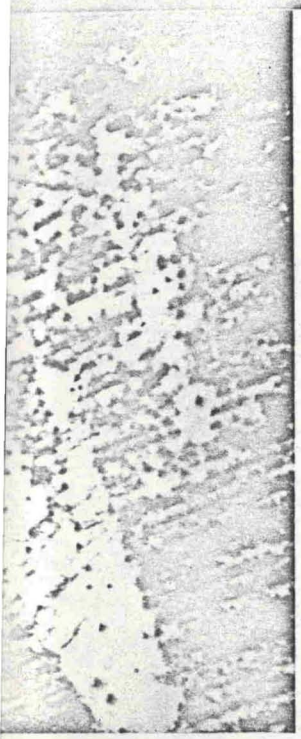

rinding and polishing; after 4 years
CH_3OH for 80 sec; 3-mm diameter
m nucleation.

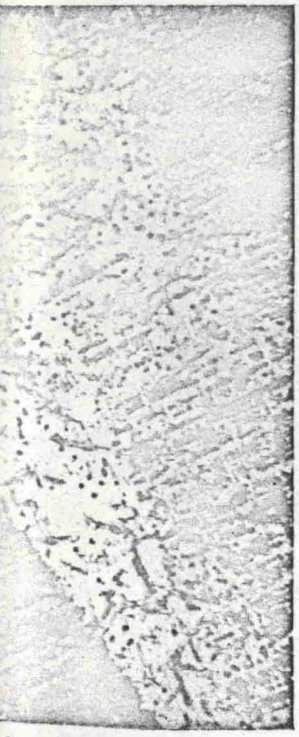

l section shown in Fig. 11; etched
$_3OH$ for 8 sec.

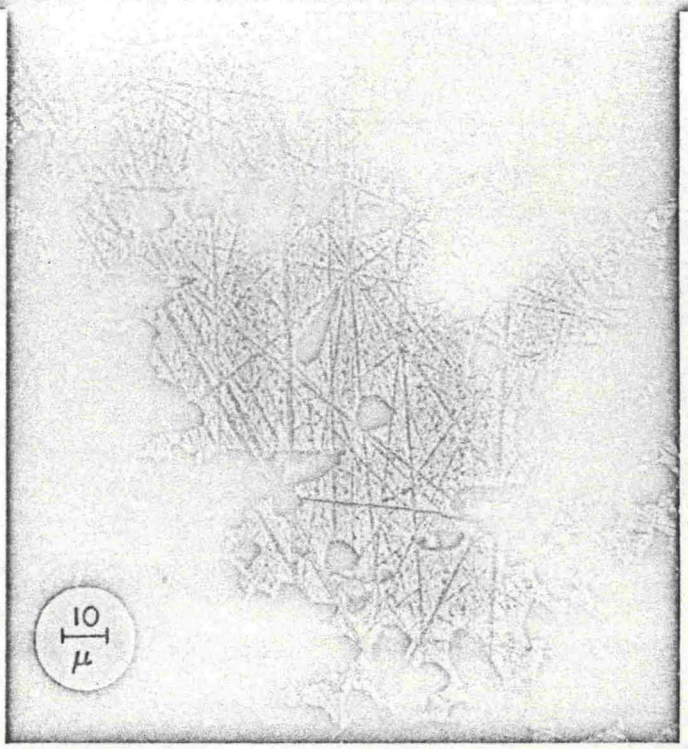

FIG. 13. Enlargement of Fig. 12 to reveal similarity to six-sided etch pits shown in Fig. 7.

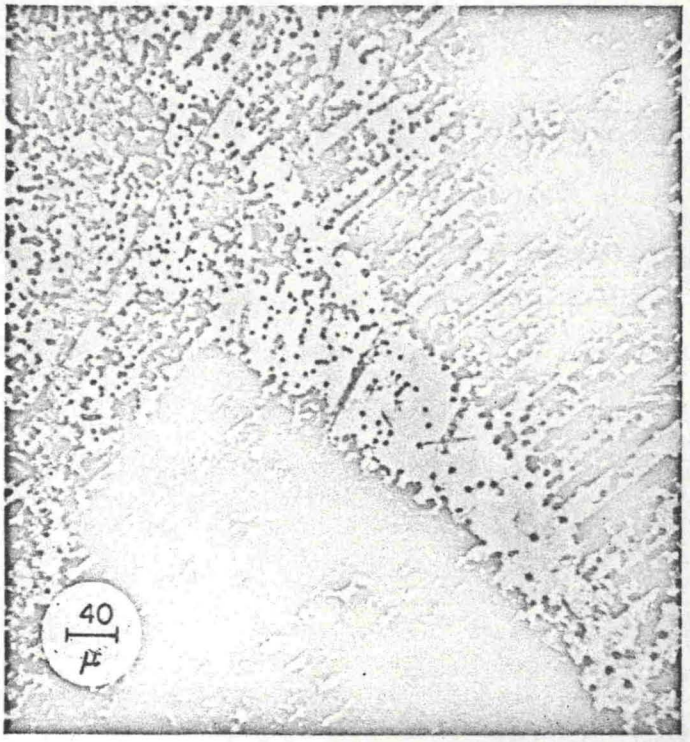

FIG. 14. Second repolishing and etching of (0001) basal section shown in Fig. 11; etched with 5 vol. % Br in CH_3OH for 8 sec.

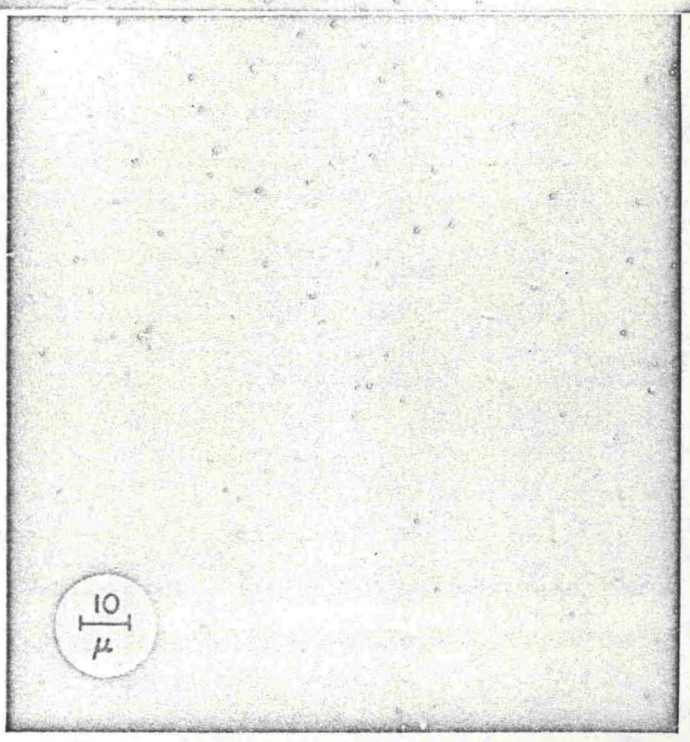

FIG. 15. (10$\bar{1}$2) cleavage face etched in 5 vol. % Br in CH_3OH for 5 sec; 10-mm diameter seeded crystal.

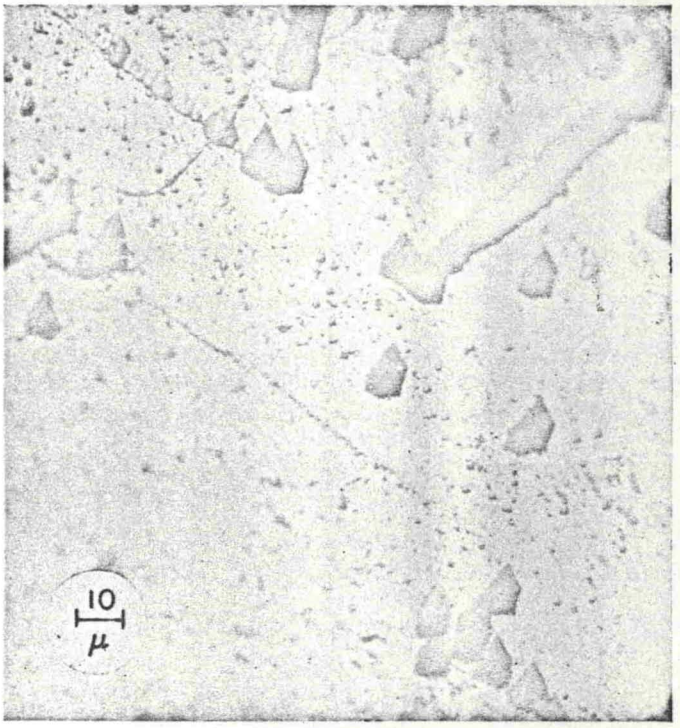

FIG. 16. (10$\bar{1}$2) cleavage face etched in 5 vol. % Br in CH_3OH for 5 sec; 3-mm diameter crystal grown by random nucleation.



FIG. 17. (10$\bar{1}$2) cleavage surface etched after one year with 5 vol. % Br in CH_3OH for 5 sec; 10 mm diameter seeded crystal.

{13$\bar{4}$1} ones. Figure 11 gives the distribution of triangular pits and Fig. 12 displays the distribution of six-sided pits obtained after repolishing. Figure 13 is an enlargement of Fig. 12 to illustrate that the pits are the same as those produced in the (0001) plane of the 10 mm crystal (Fig. 7). Repolishing and etching a third time again gave the same general distribution of etch pits (Fig. 14). Electron micrographs of replicas revealed that the pits terminated in long pipes similar to that shown in Fig. 6(b).

The effect of aging was investigated by etching a 1-year-old (10$\bar{1}$2) cleavage fragment from the same crystal that gave Fig. 15. Irregular triangular etch pits which were bisected by the ⟨11$\bar{2}$0⟩ direction formed (see Fig. 17) instead of the six-sided ones. Graphic projection of the triangular pits from the (10$\bar{1}$2) to the (0001) plane produced the {2$\bar{1}\bar{1}$3} etch pit geometry.

DISCUSSION

The diamond-shaped etch pits and the elongated grooves seen on the (10$\bar{1}$0) cleavage faces of the 10-mm diameter crystals appeared to be the sites of isolated gas bubbles and gas pipes, respectively, particularly since these

l. % Br in CH_3OH for 5 sec; 10-mm
d crystal.

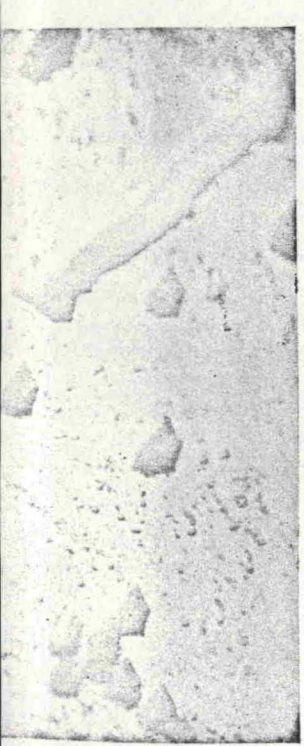

l. % Br in CH_3OH for 5 sec; 3-mm
random nucleation.

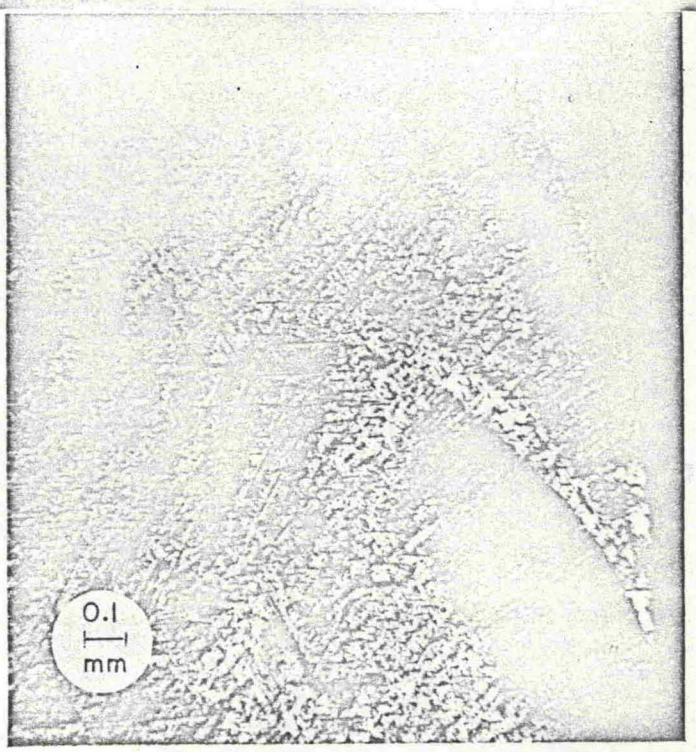

FIG. 18. (0001) basal section prepared by grinding and polishing; etched with 5 vol. % Br in CH_3OH for 8 sec; the rows of etch pits are in the $\langle \bar{1}100 \rangle$ direction; 3-mm diameter crystal grown by random nucleation.

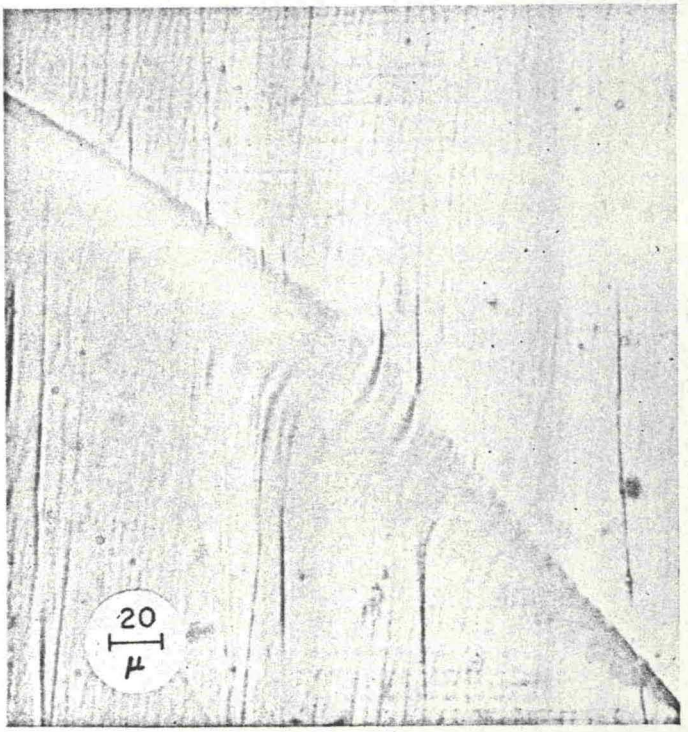

FIG. 19. Polished $(10\bar{1}0)$ cleavage face; indentor wedge at 45° to $\langle 0001 \rangle$; ripple marks are parallel to and the cracks are perpendicular to $\langle 0001 \rangle$ direction; 3-mm diameter crystal grown by random nucleation.

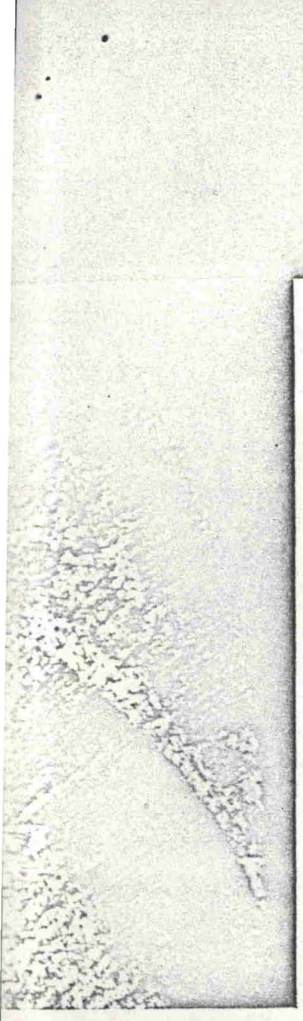

grinding and polishing; etched with
etch pits are in the ⟨$\bar{1}$100⟩ direction;
by random nucleation.

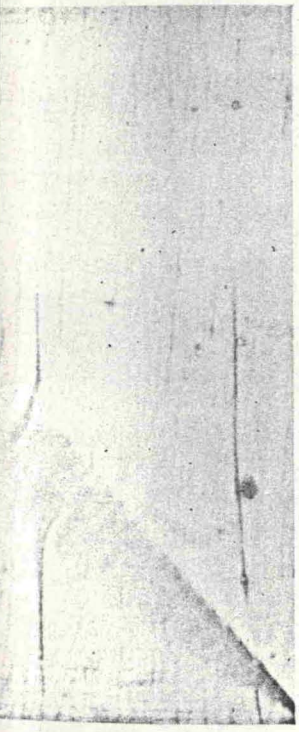

ntor wedge at 45° to ⟨0001⟩; ripple
endicular to ⟨0001⟩ direction; 3-mm
random nucleation.

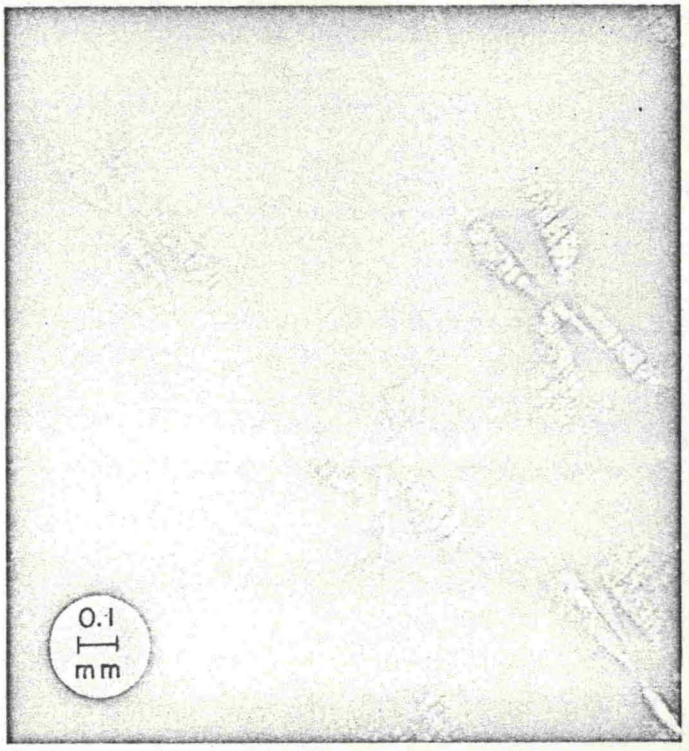

FIG. 20. Polished (10$\bar{1}$0) cleavage face; etched with 5 vol. % Br in CH_3OH for 10 sec; dark field illumination reveals preferential etching; 3-mm diameter crystal grown by random nucleation.

features were absent in the 3-mm diameter crystals and scarce in the outer 2 mm of the 10-mm diameter crystals. Elongated bubbles are frequently encountered during the freezing of water, when pipes are formed by bubble caps which move with the ice-water interface.[4]

Undoubtedly, some of the etch pits seen in the (0001) surfaces of the 10-mm diameter crystals were related to gas bubbles, but the majority must have originated from other causes since they were 10 to 100 times more numerous than gas bubbles in the (10$\bar{1}$0) plane. This conclusion is supported by the fact that an etch pit density of $\simeq 10^7/cm^2$ was found in the (0001) sections of 3-mm diameter crystals in which no gas bubbles were detected. A portion of the etch pits may have resulted from localized surface damage. The pair of mating (10$\bar{1}$2) cleavage surfaces reported earlier[1] appear to show this effect. After progressive etching only about 70 per cent of the six-sided pits could be correlated from one face to the other. The majority of these etch pits, however, appear to be due to grown-in dislocations. Evidence for dislocation motion during growth in randomly nucleated

crystals was exhibited by the rows of etch pits in the $\langle\bar{1}100\rangle$ direction separated by etch-pit-free growth bands which persisted after repeated grinding and polishing (see Fig. 18). Since dislocation motion in a plane requires that the Burgers vector lies in that plane, the indicated slip system is either $\langle\bar{1}100\rangle$ $\{11\bar{2}0\}$ or $\langle 0001\rangle$ $\{11\bar{2}0\}$ compared to $\langle 11\bar{2}0\rangle$ $\{10\bar{1}0\}$ for isostructural tellurium at room temperature.[5]

Localized strain energy which could be annealed out over long periods of time at room temperature (22°C) was revealed by the different etch-pit geometries obtained on aged versus freshly worked surfaces. Triangular etch pits similar to those seen in the present investigation were found by Eckart using a HNO_3-H_2SO_4 etchant at 150°C on the (0001) face of vapor-grown crystals.[6] He also found six-sided etch pits at 20°C in the (0001) plane of crystals grown from chlorine-doped selenium vapor. These results suggest that localized strain caused by either mechanical deformation or impurities lead to the six-sided etch pits, while the triangular pits represent a strain free surface.

No evidence was found for slip bands in the $(10\bar{1}0)$ surfaces as a result of mechanical deformation at room temperature. The orthogonal cracks and ripple marks (see Fig. 19) produced by the Knoop hardness indentor inclined at 45° to the $\langle 0001\rangle$ direction appeared to involve fracture and plastic deformation respectively. After etching, dark-field illumination showed preferential attack (Fig. 20), but the effect did not reappear after repolishing and etching. If slip bands were present as a result of plastic deformation, they should persist through repolishing and give rise to dislocation etch pits. The absence of dislocation etch pits in the $(10\bar{1}0)$ plane, however, may be due to the insensitivity of the etchant on this surface.

ACKNOWLEDGMENT

The authors are indebted to Mr. J. E. Hudson and Dr. R. W. Armstrong for preparing the standard projections, to Miss Jean Coles for the electron photomicrographs and to Dr. F. F. Lange for his helpful discussions.

REFERENCES

1. Harrison, J. D. and Sagar, A., *J. Appl. Phys.* **38**, 3791 (1967).
2. Harrison, D. E. and Tiller, W. A., *J. Appl. Phys.* **36**, 1680 (1965).
3. Harrison, J. D., *J. Appl. Phys.* **39**, 3672 (1968).
4. Chalmers, B., *Scientific Am.* **200**, 114 (1959).
5. Stokes, R. J., Johnston, T. L. and Li, C. H., *Acta Met.* **9**, 415 (1961).
6. Eckart, F., *Recent Advances in Selenium Physics*, Pergamon, London, 1965.